

Introduction, Aims and Methods

Despite the increase in incidence there are still no prognostic biomarkers able to identify high-risk subsets of AJCC Stage I/II melanomas. We have recently identified the immunohistochemical expression of Autophagy and beclin 1 regulator 1 (AMBRA1) and lorcin in the epidermis overlying early-stage primary AJCC I melanomas as a robust prognostic biomarker. However, despite this advance the process of scoring histological images remains labour intensive and influenced by subjectivity.

Artificial intelligence (AI) has improved the accuracy of several pattern recognition tasks and has shown good results even for tasks previously considered too challenging to be accomplished with conventional image analysis methods.

The purpose of this pilot study was to develop and use optimised algorithms within Visiopharm image analysis to determine AMBLor expression in a cohort of 36 histological image of non-ulcerated AJCC stage I/II melanomas derived Buffalo, USA and compare with scoring analysis a determined using a current binary scoring system by Histopathologists (Figure 1).

Figure 1

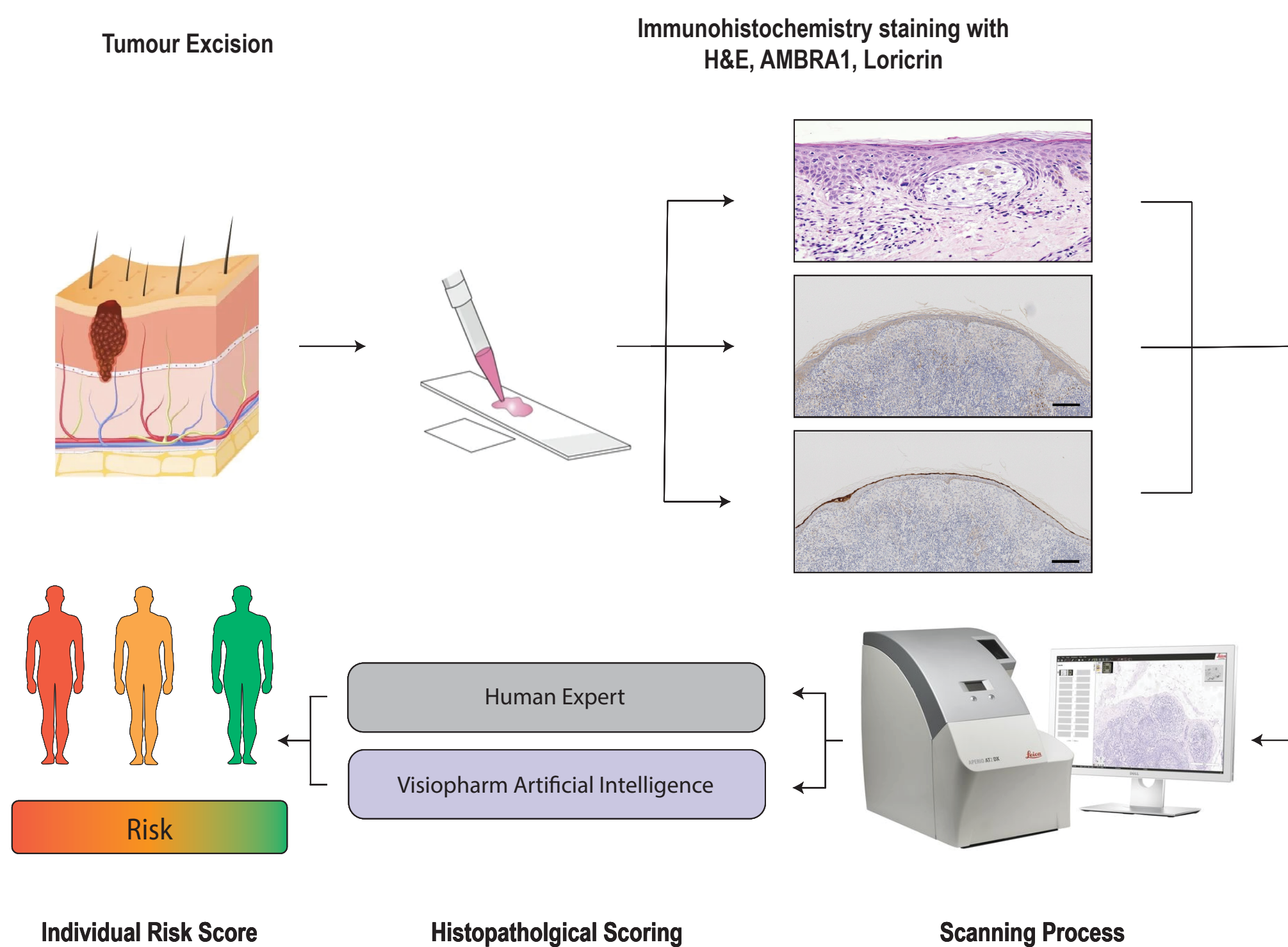


Figure 1 | Workflow demonstrating the process and analysis of Stage I/II Malignant Melanoma from tumour excision to individual risk scoring. Melanomas were excised from 12 patients in Buffalo, USA. Three automated immunohistochemistry stains were performed (hematoxylin and eosin, AMBRA1 and Lorcin). 36 slides were scanned using a Leica Biosystem Aperio A2 scanner (X20 magnification). Using VIS, Visiopharm AI platform version 2019.07.03 a deep learning-based classifier was trained to identify high/low risk tumour subsets and compared to a consensus of Histopathologists (Human Expert).

Figure 2

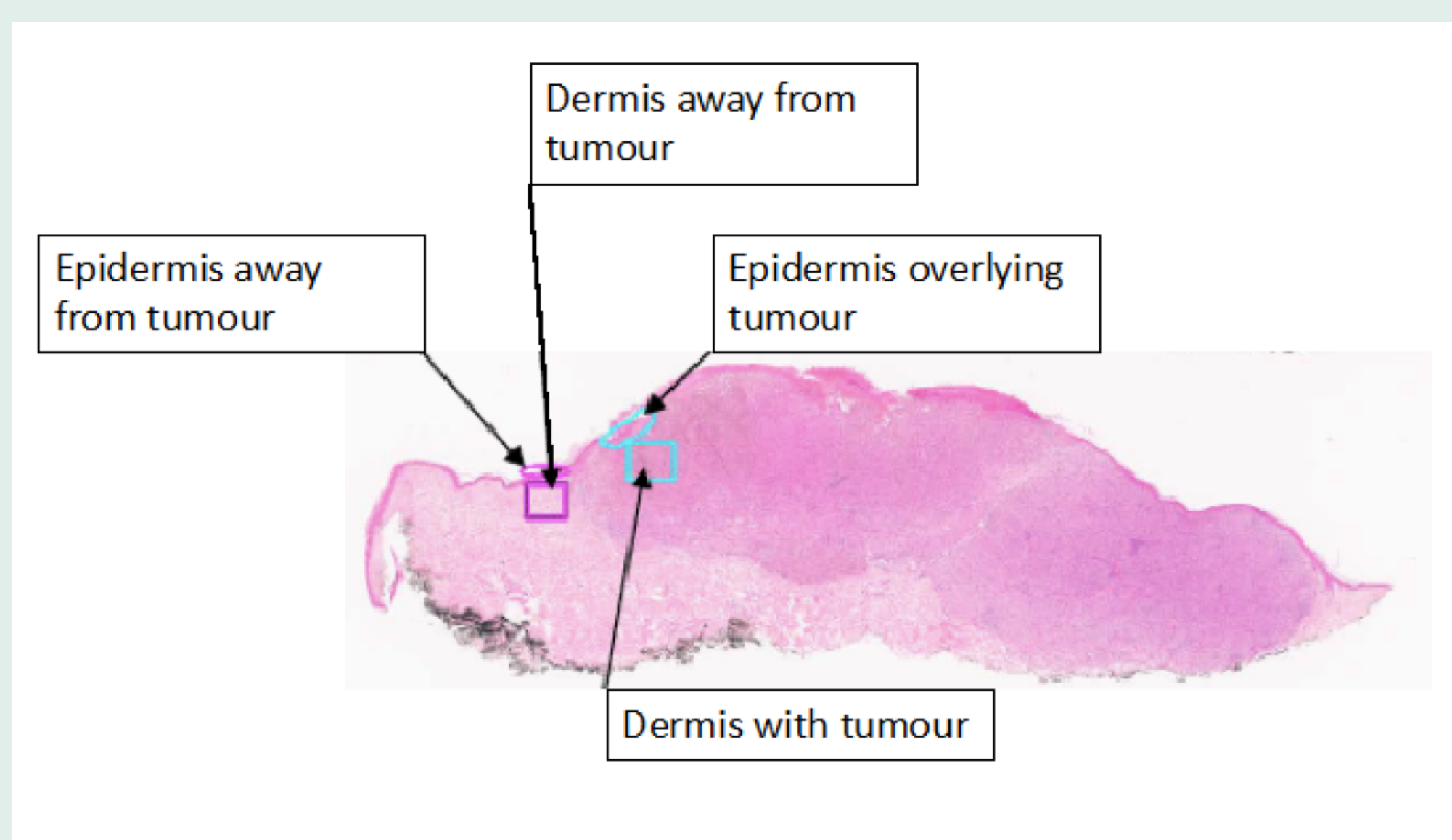


Figure 2 | Annotated H&E histological digital image of a non-ulcerated melanoma depicting; Pink circle- Normal Epidermis, Pink square- Normal Dermis, Blue circle- Tumour Epidermis, Blue Square- Tumour Dermis. Scale bar = 1mm.

Figure 3

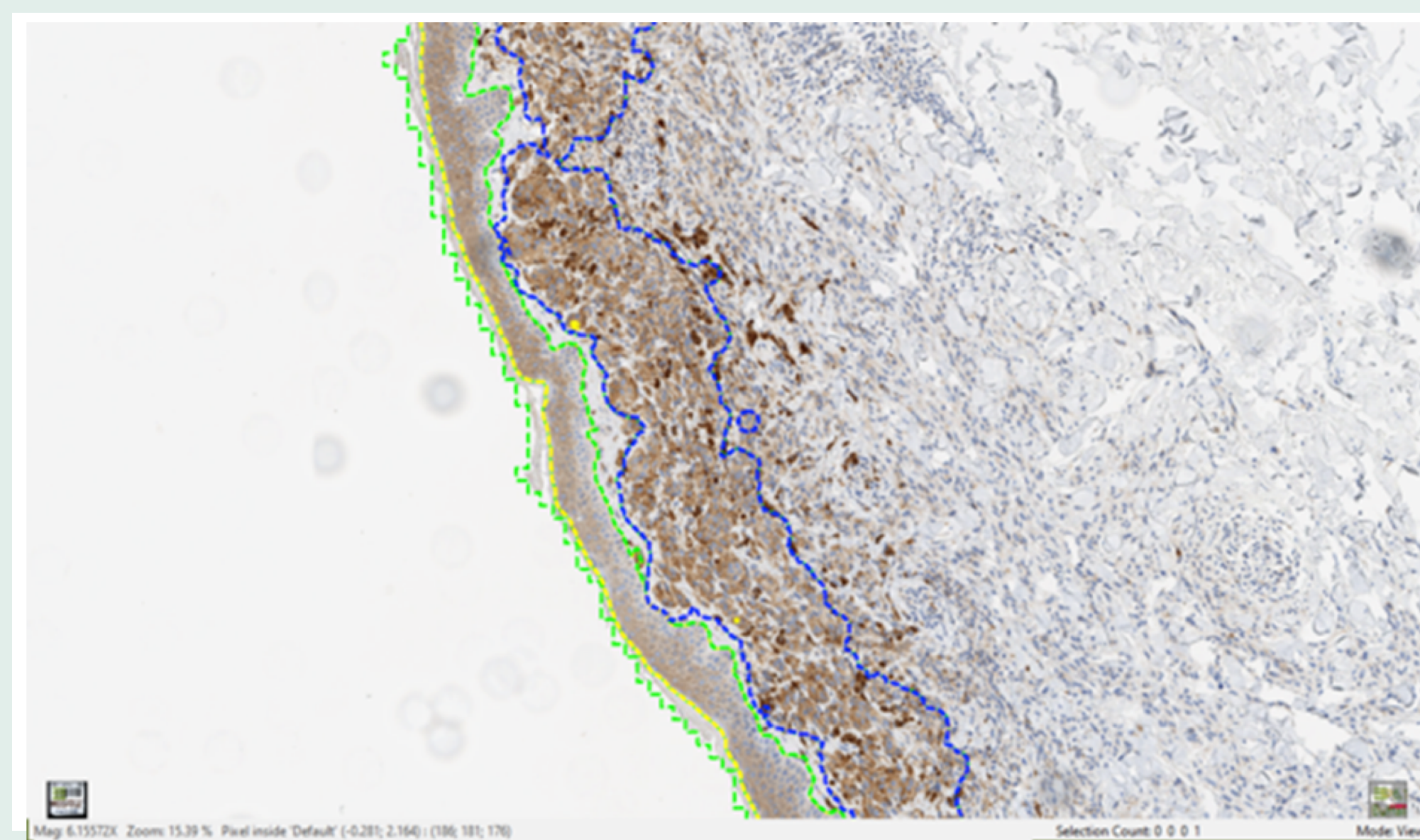


Figure 3 | Representative images depicting Regions of Interest for AMBRA1/Lorcin algorithm development. Blue dashed line- melanoma/Tumour Dermis, yellow dashed line- skin surface (overlay from H&E image), green dashed line- tumour epidermis. Scale bars = 100µm.

Figure 4

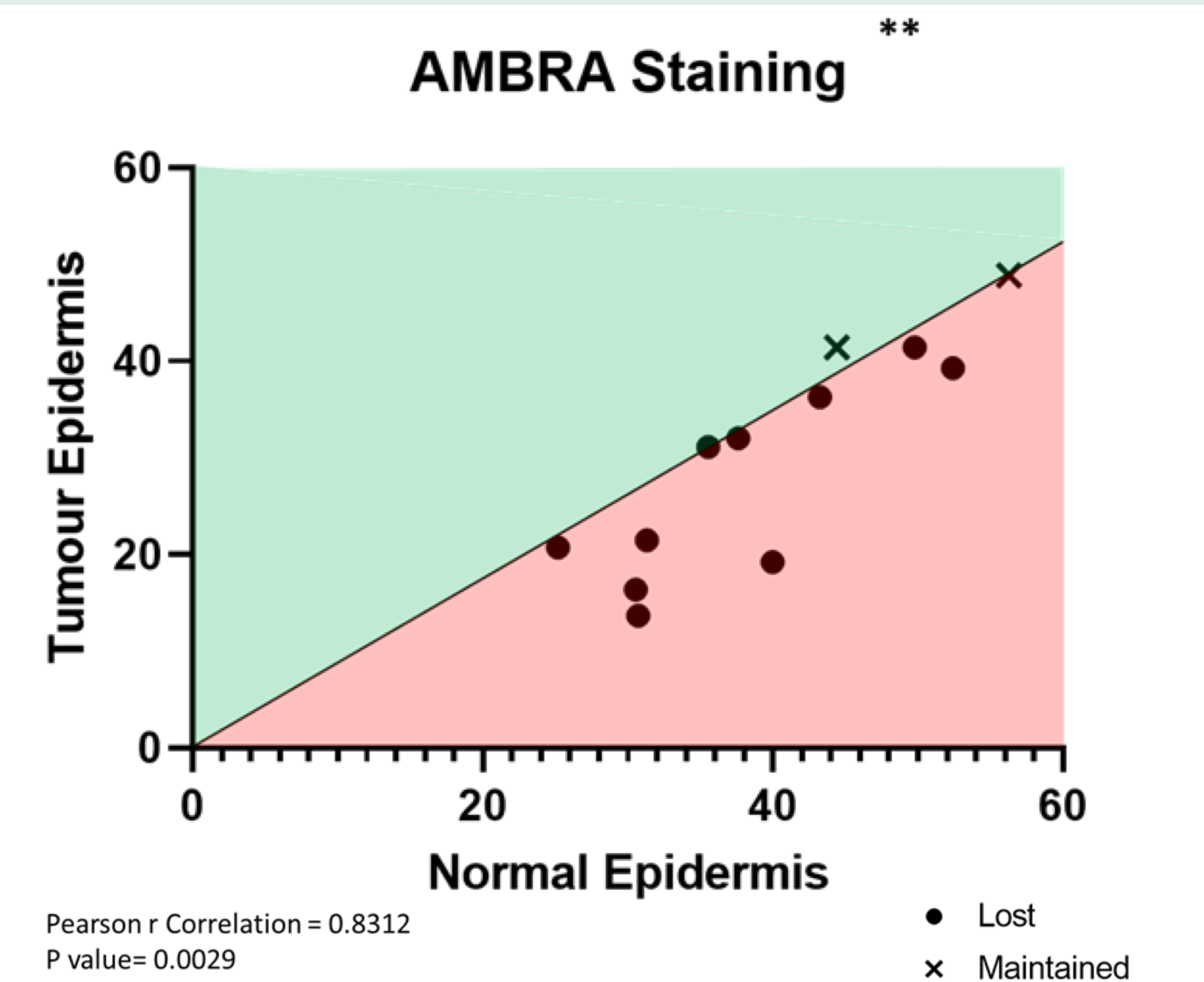


Figure 4 | Scatter plot of epidermal AMBRA1 expression overlying cases of primary melanoma compared to expression in the normal epidermis. Values which lie in the green (area above the curve) indicate those melanomas with maintained epidermal AMBRA1 expression, whereas values in red (area below the curve) indicate those in which AMBRA1 expression is lost (Pearson r Correlation = 0.8312, p value= 0.0029).

Figure 5

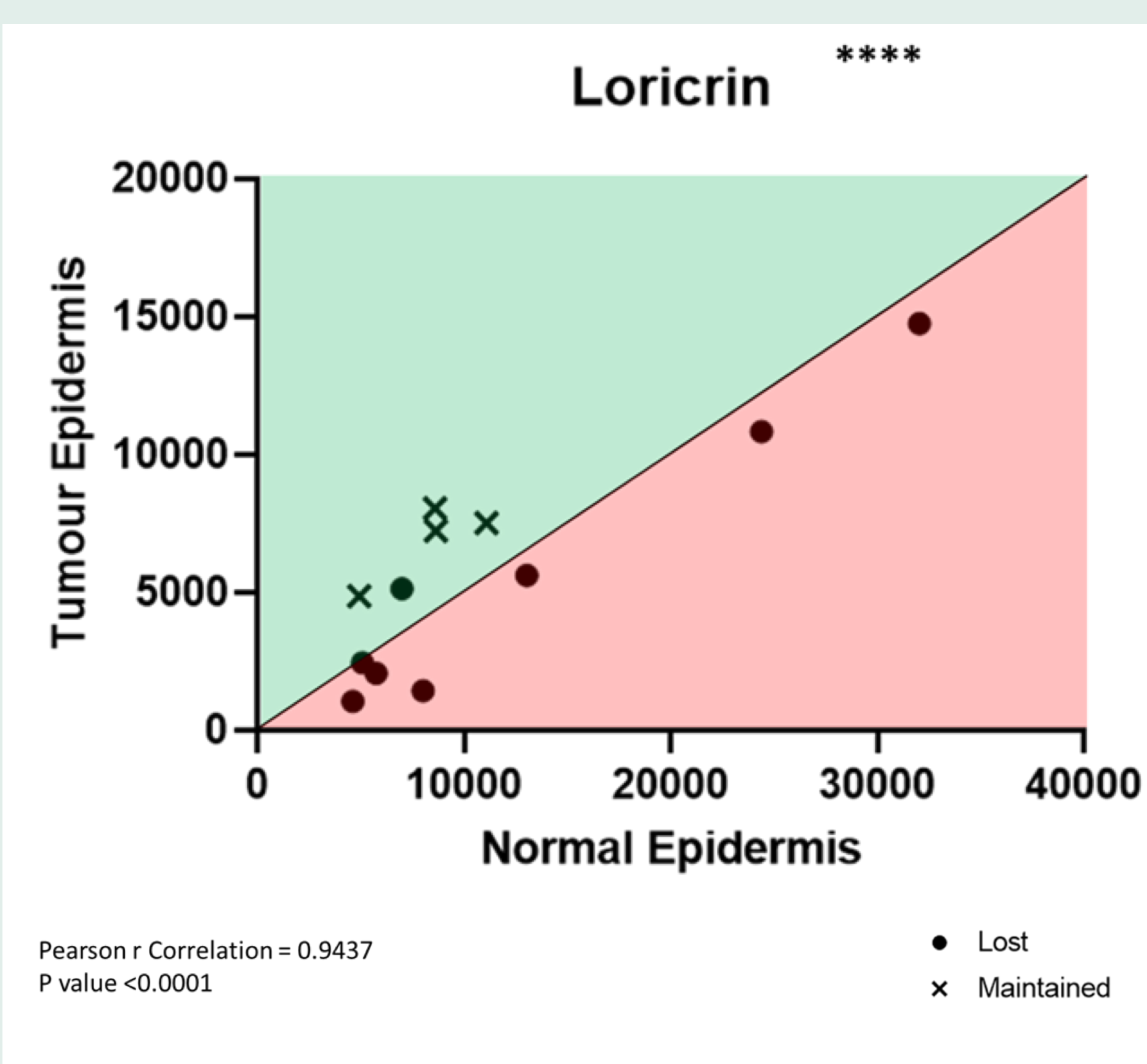


Figure 5 | Scatter plot of epidermal Lorcin expression overlying cases of primary melanoma compared to expression in the normal epidermis. Values which lie in the green (area above the curve) indicate those melanomas with maintained epidermal Lorcin expression, whereas values in red (area below the curve) indicate those in which epidermal Lorcin expression is lost (Pearson r Correlation = 0.9437, p value<0.0001).

Figure 6

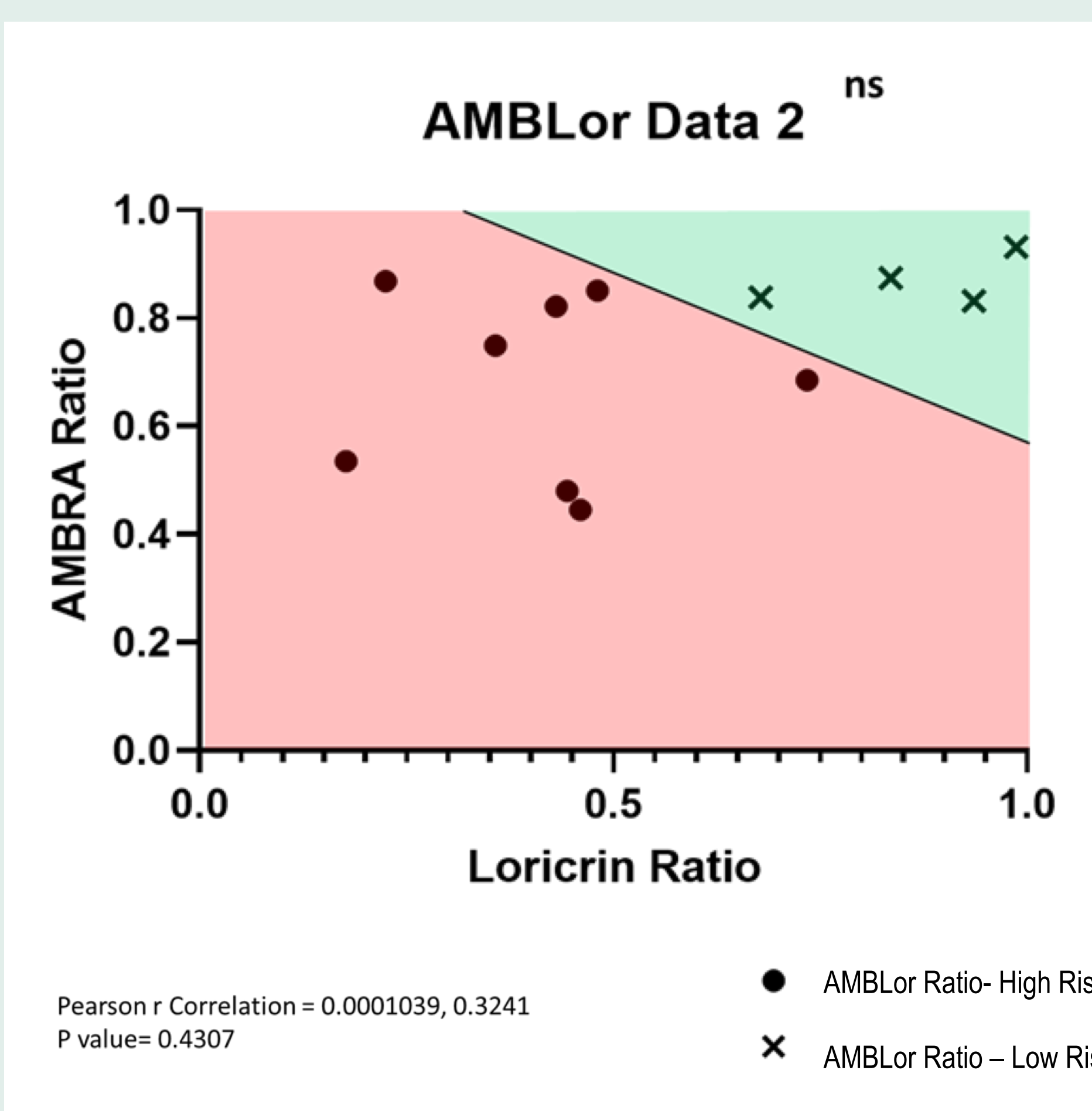


Figure 6 | Scatter plot demonstrating AMBLor Score of Lorcin Ratio compared to AMBRA1 ratio. Values which lie in the green (area above the curve) should have low risk AMBLor Ratio, whereas values in red (area below the curve) should have a high risk AMBLor Ratio (Pearson r Correlation = 0.0001039, 0.324, p value = 0.4307). Dots= high risk AMBLor Ratio according to histopathological assessment and, crosses= low risk AMBLor Ratio according to histopathological assessment.

Figure 7

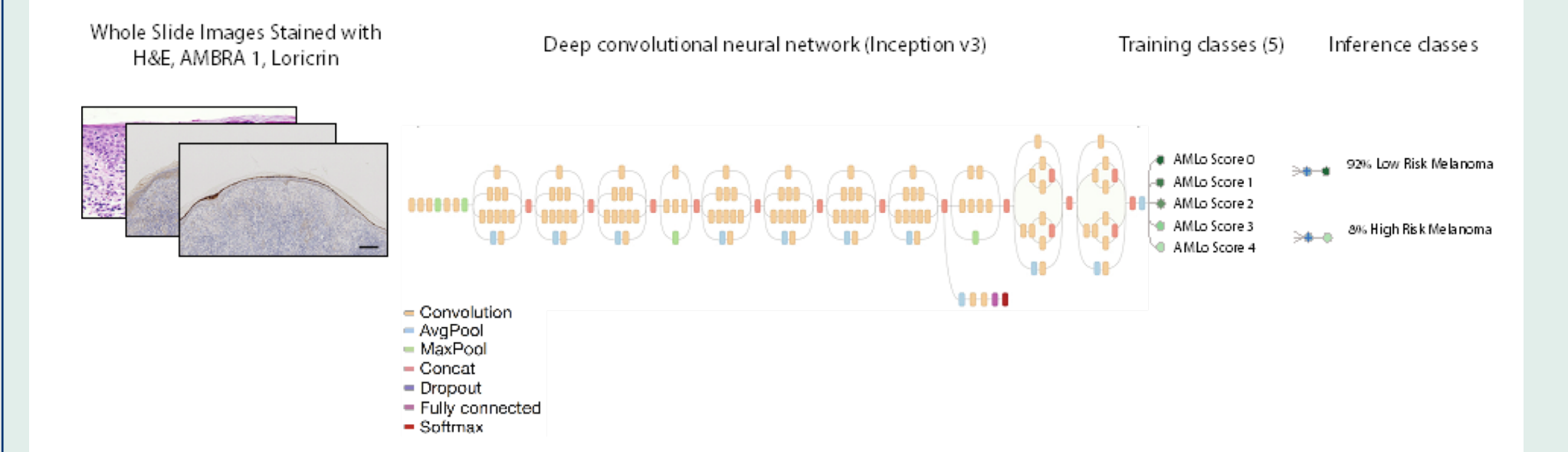


Figure 7 | Deep CNN layout. Data flow is from left to right: an image of a whole slide image is sequentially warped into a probability distribution over clinical classes of skin disease using Google Inception v3 CNN architecture pretrained on the ImageNet dataset (1.28 million images over 1,000 generic object classes) and fine-tuned on our own dataset of 1,000 histological slides comprising 5 different disease classifications. Inference classes are more general and determine high risk and low risk melanomas. The probability of an inference class is calculated by summing the probabilities of the training classes according to taxonomy structure.

Results

Visiopharm image analysis software identified regions of interest within the histological H&E images, specifically the tumour, epidermis and dermis. (Figure 3)

We then identified multiple auxiliary analysis protocol packages to quantitatively analyse scanned AMBRA 1, Lorcin and Haematoxylin and eosin stains. Results revealed a strong correlation between mean tumour epidermal AMBRA1 density and groups with Lost or Maintained AMBRA expression (Figure 4), with similar results found for peritumoural epidermal Lorcin expression (Figure 5). Interestingly, we additionally identified an association between loss of combined epidermal AMBRA/Lorcin expression with a high-risk sub-group (Figure 6), suggesting Visiopharm as a viable means to determine AMBLor expression.

Further studies are aimed at using optimised algorithms within Visiopharm to determine AMBLor expression in larger independent cohorts of non-ulcerated AJCC stage I/II melanomas and to investigate the potential for this approach to predict 5-year disease free survival of patients. In addition, alternative approaches to harness Artificial intelligence to evaluate AMBLor as a prognostic biomarker for AJCC stage I/II melanoma will incorporate the development of a bespoke neural network platform using the Inception V3 network (Figure 7).

Acknowledgements

Cancer Research UK
 North Eastern Skin Research Fund
 AMLO Biosciences

References

- 1) Ellis R, Tang D, Nasr B, et al. Epidermal autophagy and beclin 1 regulator 1 and lorcin: a paradigm shift in the prognostication and stratification of the American Joint Committee on Cancer stage I melanoma. *Br J Dermatol*. 2020.
- 2) Esteva A, Kuprel B, Novoa RA, et al. Dermatologist-level classification of skin cancer with deep neural networks. *Nature* 2017. *Acad Sci U S A*. 2015;112(32):9920-9925.